

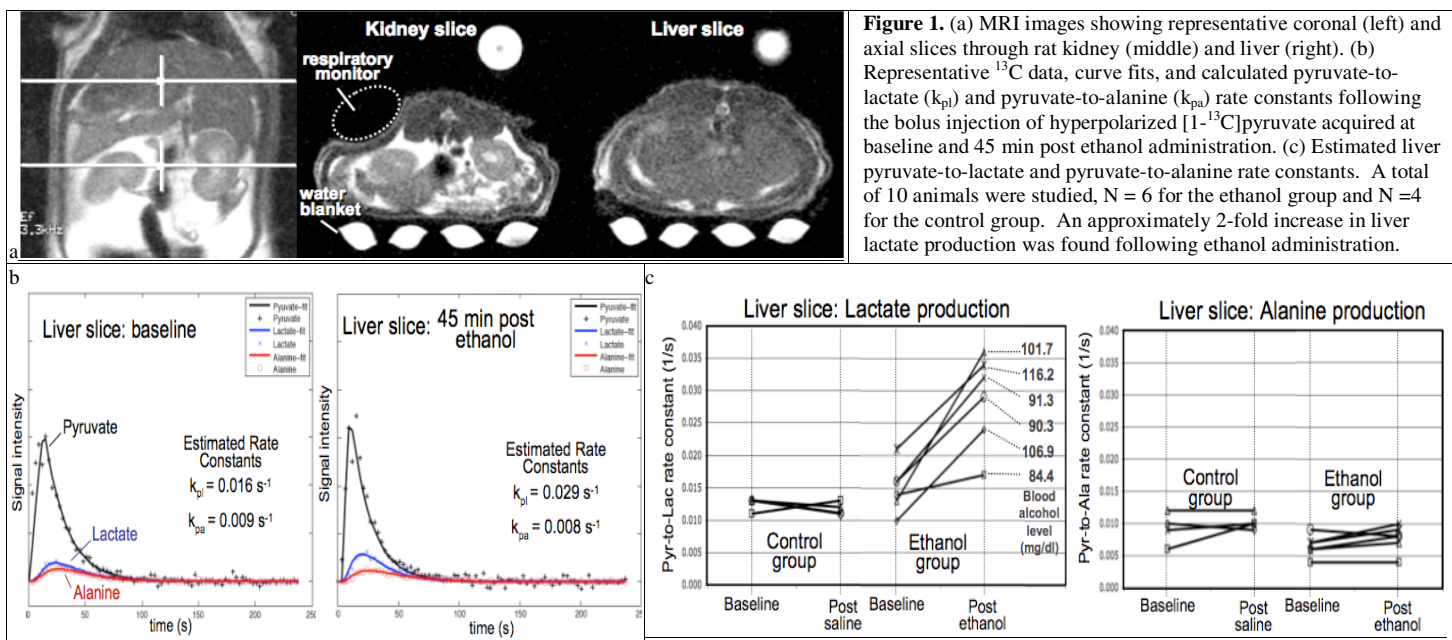
## In Vivo Hyperpolarized <sup>13</sup>C-MRS of Ethanol-Modulated Pyruvate Metabolism in the Rat

D. M. Spielman<sup>1</sup>, D. Mayer<sup>1,2</sup>, Y-F. Yen<sup>3</sup>, J. Tropp<sup>4</sup>, R. E. Hurd<sup>3</sup>, and A. Pfefferbaum<sup>2,5</sup>

<sup>1</sup>Radiology, Stanford University, Stanford, CA, United States, <sup>2</sup>SRI International, Menlo Park, CA, United States, <sup>3</sup>GE Healthcare, Menlo Park, CA, United States, <sup>4</sup>GE Healthcare, Fremont, CA, United States, <sup>5</sup>Psychiatry and Behavioral Sciences, Stanford University, Stanford, CA, United States

**Introduction:** This work demonstrates the application of *in vivo* MRS of hyperpolarized [ $1-^{13}\text{C}$ ]pyruvate to interrogate a metabolic pathway involved in neither glycolysis nor the Krebs cycle. In particular, ethanol is metabolized in the liver via the breakdown of ethanol to acetaldehyde and acetaldehyde to acetate. These reactions are catalyzed by the enzymes alcohol dehydrogenase (ADH) and acetaldehyde dehydrogenase (ALDH), with both requiring the reduction of the coenzyme nicotinamide adenine dinucleotide ( $\text{NAD}^+$ ) to  $\text{NADH}$  [1]. Hence, ethanol consumption leads to an accumulation of excess  $\text{NADH}$  in the liver and when extreme is associated with pathologies including fatty liver disease, hepatitis, cirrhosis, and hepatocellular carcinoma [2]. Here we present a method for noninvasively monitoring this important process *in vivo*. Using a bolus injection of hyperpolarized [ $1-^{13}\text{C}$ ]pyruvate, we demonstrate significantly increased rat liver lactate production with the co-administration of ethanol, an effect attributable to increased liver  $\text{NADH}$  in combination with  $\text{NADH}$ 's role as a coenzyme in pyruvate-to-lactate conversion [3,4].

**Methods:** Ten male Wistar rats ( $370 \pm 21$  g) were anesthetized with 1-3% isoflurane and fitted with a tail vein catheter for administration of ethanol (or saline) and pyruvate. Using a DNP polarizer (HyperSense™, Oxford Instruments), we polarized a  $32\mu\text{l}$  formulation of 14 M [ $1-^{13}\text{C}$ ]pyruvate for each injection. The frozen sample was dissolved in 4.6 cc of  $185^\circ\text{C}$  buffered NaOH, yielding a 100 mM pyruvate solution ( $\text{pH} = 7.4 \pm 0.34$ ) hyperpolarized to approximately 20%. Each rat was placed in an 80-mm inner-diameter dual-tuned  $^{13}\text{C}$ - $^1\text{H}$  volume RF coil centered in the bore of a 3T clinical MR scanner (GE Healthcare, Waukesha, WI). After the acquisition of conventional MRI for anatomical reference, 2.5 cc of hyperpolarized pyruvate solution was injected into the tail vein catheter at a rate of  $0.25 \text{ ml/s}$ .  $^{13}\text{C}$  spectra (FID acquisition, flip angle =  $5^\circ$ , 5kHz spectral width, 2048 points) were then acquired every 3 s over a 4-minute period from a single 15-mm axial slice through the liver ( $N=3$ ) or one slice through the liver and a second through kidneys ( $N=3$ ). Following the acquisition of the baseline pyruvate measurements, 1.0 gm/kg of a 20% ethanol solution was injected into the tail vein in order to achieve a targeted steady-state blood alcohol level of 100 mg/dl at the time of the second  $^{13}\text{C}$  MRS acquisition. A second bolus of hyperpolarized pyruvate was injected into the animal 45 min after the administration of the ethanol, and  $^{13}\text{C}$  spectra were again acquired every 3 s over the next 4 minutes. Control animals ( $N = 4$ ) were scanned using the same procedures with the exception that the ethanol injection was replaced by an injection of normal saline (same volume and temperature as the ethanol injection). The time-resolved metabolic signals following each bolus injection were fit using a three-site exchange model in order to estimate the apparent rate constants. Statistical analysis of the data was performed using two-factor repeated-measures ANOVA.



**Results:** Representative  $^1\text{H}$ -MRI images from a control animal, indicating selected slice locations, are shown in Fig. 1a. Because the  $^{13}\text{C}$  MRS data were not spatially localized within a given slice, the liver and kidney slices contained vascular and other structures in addition to the targeted organs. Hence, the dynamic MRS spectra should be considered as estimates of the true temporal variations of the organ-specific metabolite levels. Fig. 1b shows representative liver pyruvate, lactate, and alanine levels versus time curves, computed by peak integration of the spectra acquired at baseline and 45 min post-ethanol injection. Increased lactate signal post-relative to pre-ethanol injection is clearly visible. Using a three-site exchange model, we estimated the apparent pyruvate-to-lactate and pyruvate-to-alanine metabolic rate constants from the liver ( $N = 6$ ) and kidney ( $N = 3$ ) slices pre- and post-ethanol injection and pre- and post-saline injection (controls,  $N = 4$ ) (see Fig 1c). In the liver, the ethanol treated group showed a significant increase between the baseline and post-ethanol lactate production rates ( $P = 0.0016$  unpaired t-test,  $P = 0.01$  Mann-Whitney U) but no alanine differences. Lactate production, following the ethanol injection, increased by a factor of 2.0 ( $\pm 0.5$  s.e.m.). The kidney slice showed only a trend toward increased post-ethanol lactate production ( $P = 0.047$  unpaired t-test,  $P = 0.077$  Mann-Whitney U). By contrast, no significant changes were found in the control group. Smaller effects are expected for the kidney because rat kidney ADH levels are  $1/30^{\text{th}}$  of those in the liver [5]. However, statistical inferences with respect to the kidney data should be viewed with caution due to the small sample size. Final blood alcohol levels ranged from 84.4 to 116.2 mg/dl.

**Discussion:** This rodent model produces a large reproducible change in liver lactate production with minimal changes detected in liver alanine, kidney lactate, and kidney alanine, demonstrating that the rate limiting step for the conversion of pyruvate to lactate in rat liver is not LDH activity but rather NADH availability. From a technical development perspective, measurement of the conversion of pyruvate to lactate as modulated by ethanol is an ideal animal model to validate new *in vivo* hyperpolarized  $^{13}\text{C}$ -MRS/MRSI pulse sequences and associated metabolic modeling algorithms. These data also provide initial insights into liver metabolism *in vivo* at the systems level, potentially applicable to alcoholism-induced conditions including alcoholic fatty liver disease, alcoholic hepatitis, liver cirrhosis and liver cancer. Viewed as an indirect assay of changes in NADH levels, hyperpolarized  $^{13}\text{C}$ -pyruvate can potentially be useful for interrogating any of the large number of *in vivo* metabolic pathways involving the coenzyme  $\text{NAD}^+/\text{NADH}$ .

**References:** [1] Berg, et al., *Biochemistry*. 2006; W.H. Freeman. [2] Randi, et al., *Ann Oncol*, 2005, 16(9): p. 1551-5. [3] Jue, et al., *PNAS*, 1985, 82(16): p. 5246-9. [4] Forsander, et al., *Acta Chem Scand*, 1965, 19(7): p. 1770-1. [5] Tussey, et al., *PNAS*, 1989, 86(15).

**Acknowledgements:** Lucas Foundation & NIH grants RR09784, CA114747, AA005965, and U01 AA013521 (INIA).